

Electronic Supplementary Information

**Novel ferrocenyl functionalised phosphinecarboxamides:
synthesis, characterisation and coordination**

Michal Navrátil,^a Erica N. Faria,^b Geve Panahy,^b Ivana Císařová,^a
Jose M. Goicoechea^{b*} and Petr Štěpnička^{a*}

1. Additional structural diagrams

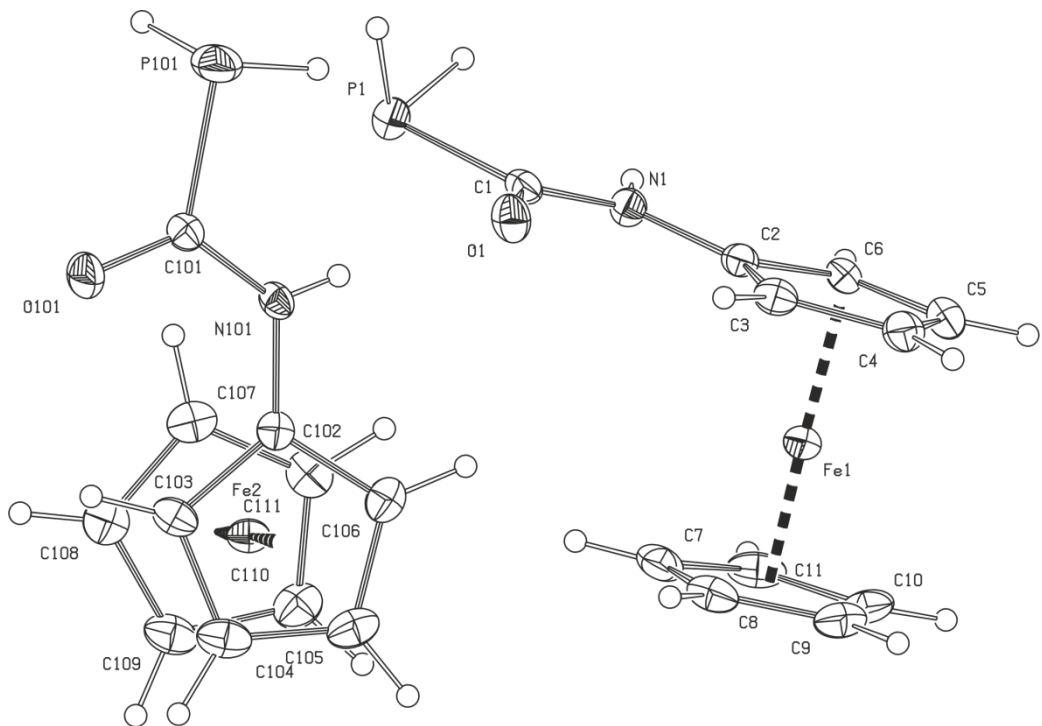


Figure S1. PLATON plot of the molecular structure of **1** showing atomic labels and displacement ellipsoids at the 30% probability level.

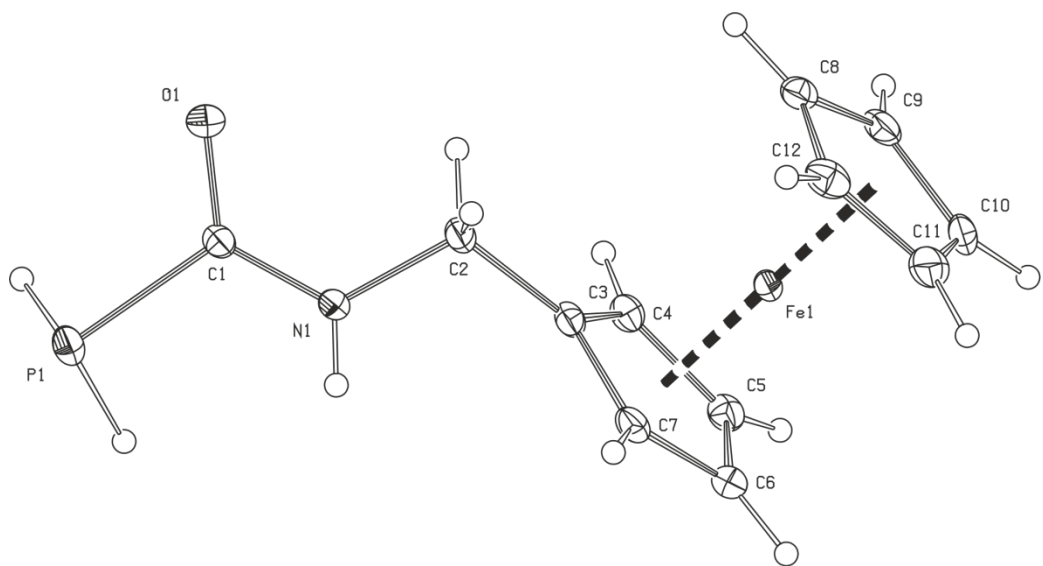


Figure S2. PLATON plot of the molecular structure of **2** showing atomic labels and displacement ellipsoids at the 30% probability level.

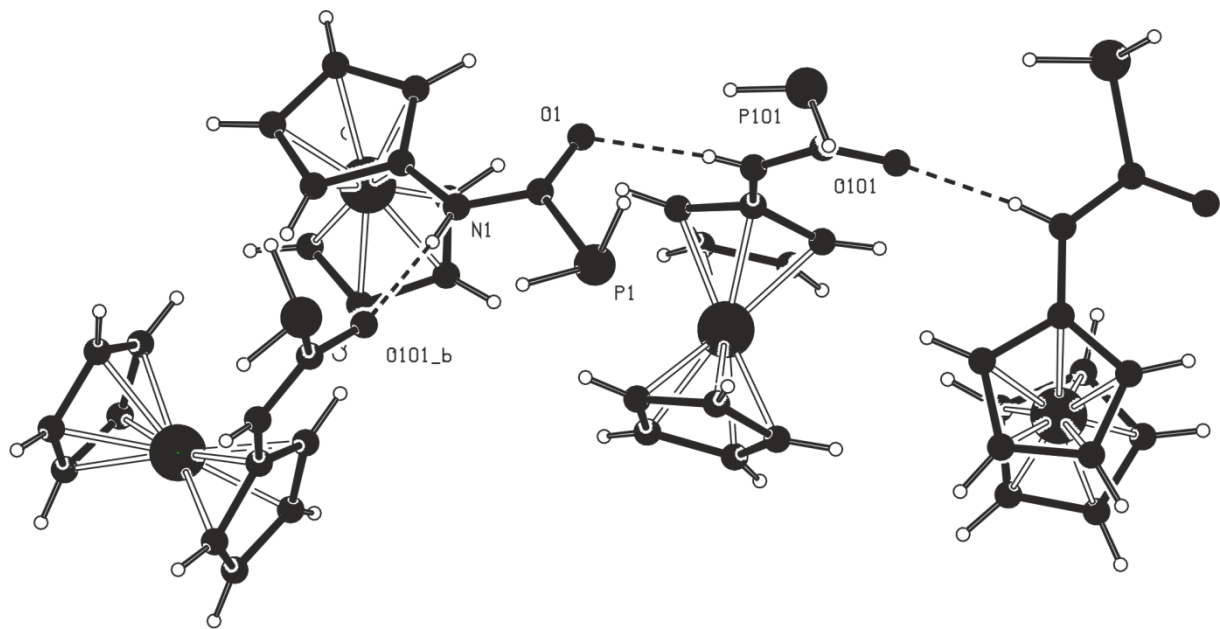


Figure S3. Section of the hydrogen-bonded chains in the structure of **1**.

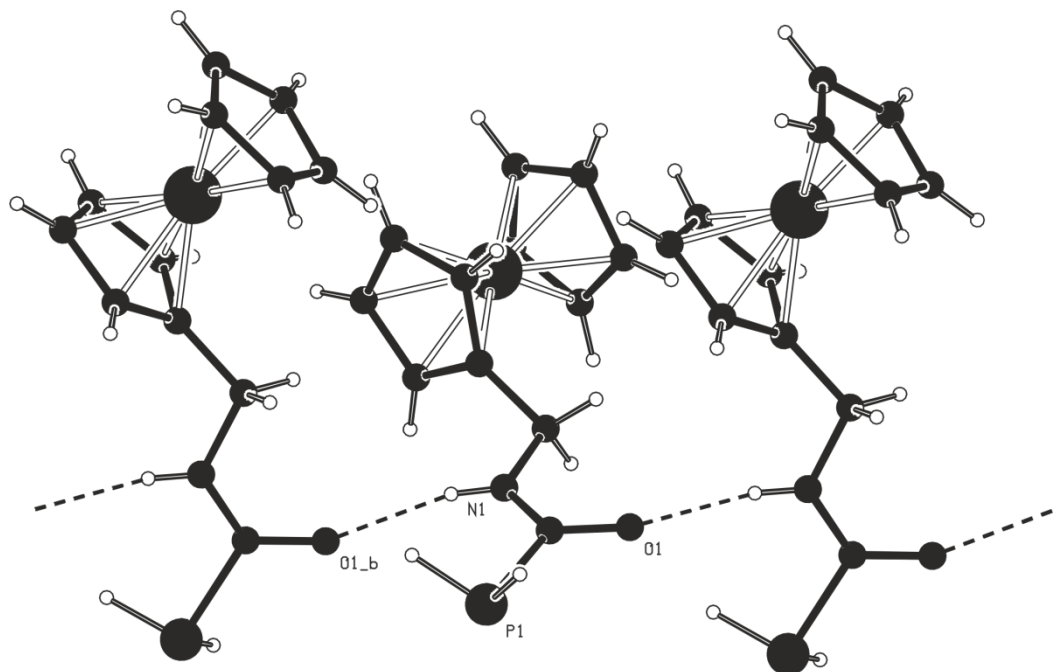


Figure S4. Section of the hydrogen-bonded chains in the structure of **2**.

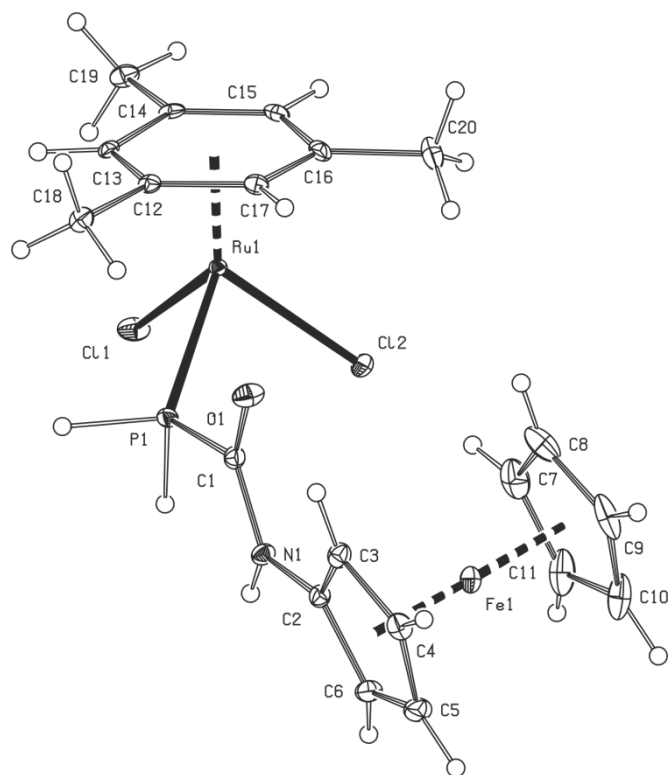


Figure S5. PLATON plot of the molecular structure of $\mathbf{3}^{\text{Ru}}$ showing atomic labels and displacement ellipsoids at the 30% probability level.

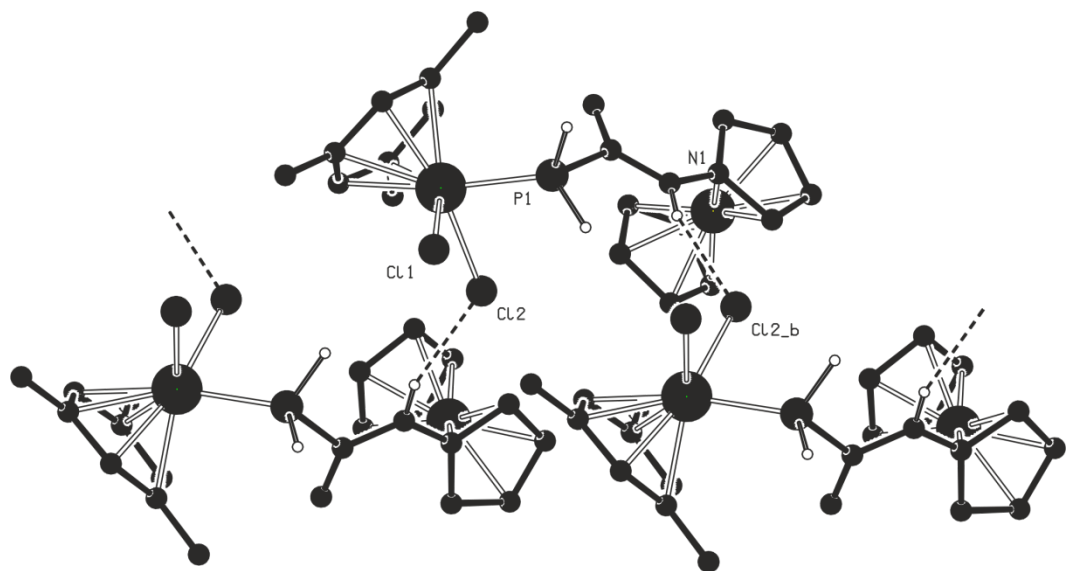


Figure S6. Section of the hydrogen-bonded chains in the structure of $\mathbf{3}^{\text{Ru}}$. Only the NH and PH hydrogens are shown for clarity.

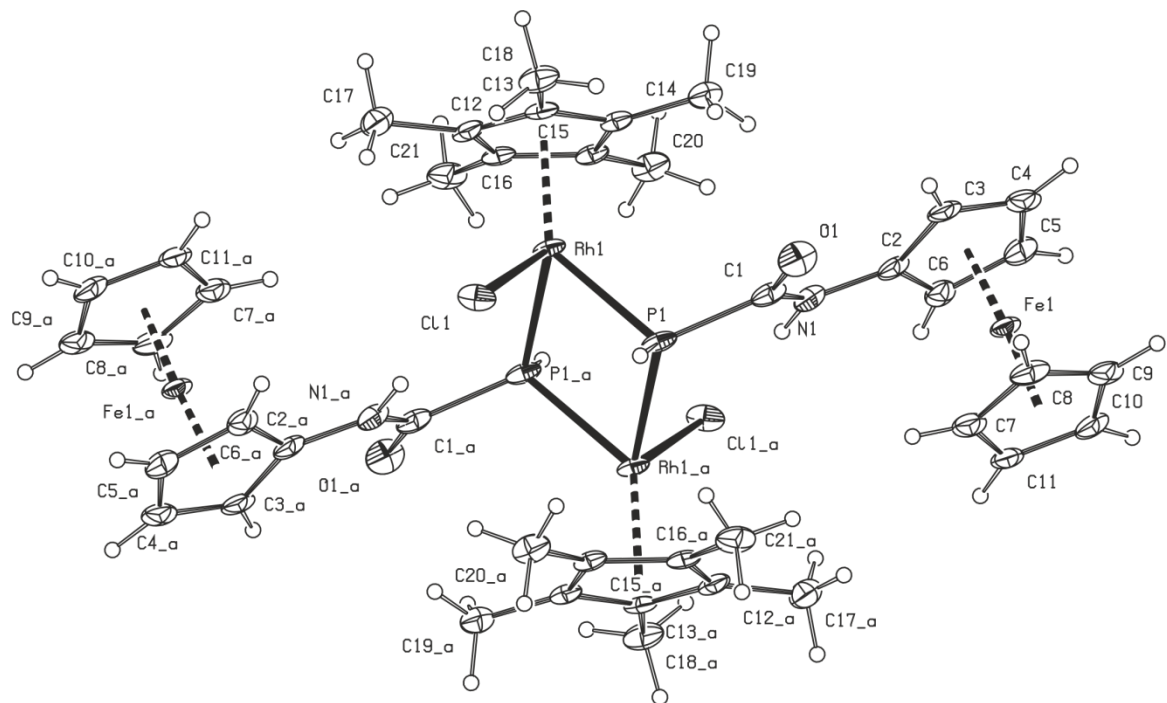


Figure S7. PLATON plot of the molecular structure of *anti*-4^{Rh}. Displacement ellipsoids enclose the 30% probability level.

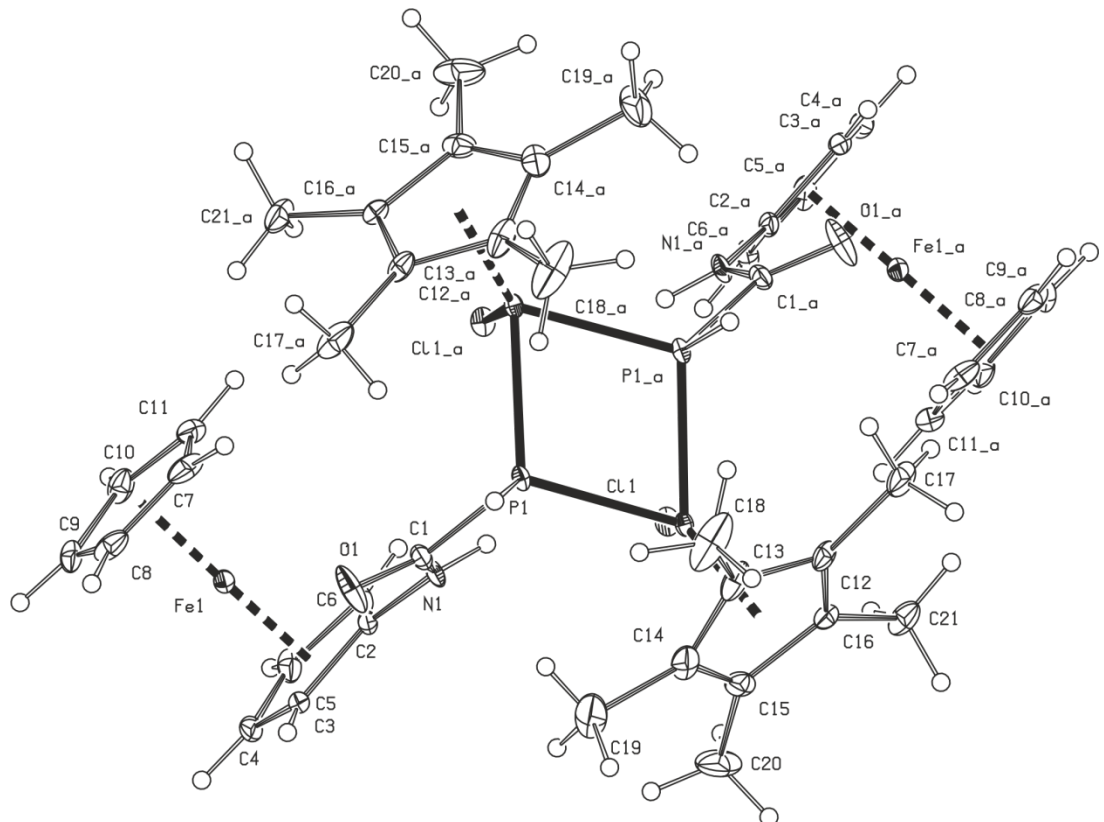


Figure S8. PLATON plot of the molecular structure of *syn*-4^{Rh}. Displacement ellipsoids enclose the 30% probability level.

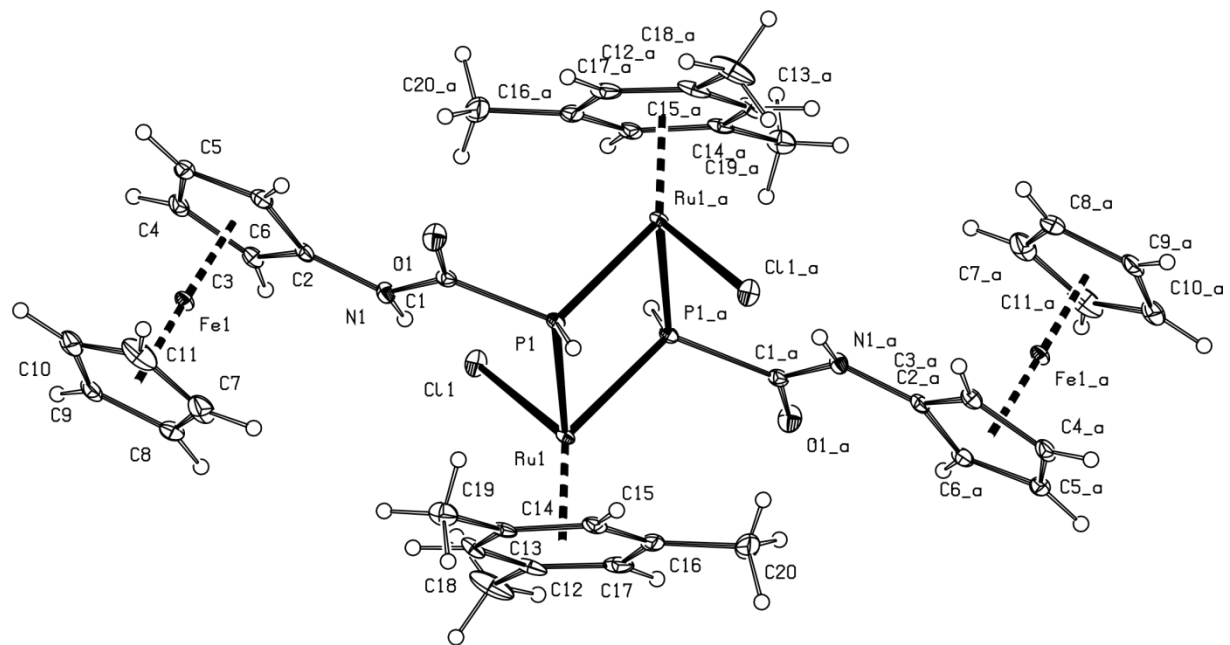


Figure S9. PLATON plot of the molecular structure of *anti*-4^{Ru} with displacement ellipsoids at the 30% probability level.

2. Summary of crystallographic data and structure refinement parameters

	1	2
Empirical formula	C ₁₁ H ₁₂ FeNOP	C ₁₂ H ₁₄ FeNOP
Formula weight	261.04	275.06
Temperature/K	150(2)	150(2)
Crystal system	monoclinic	orthorhombic
Space group	<i>P</i> 2 ₁ / <i>c</i>	<i>P</i> bca
a/Å	15.9398(5)	9.6692(2)
b/Å	7.9962(3)	9.2447(2)
c/Å	17.9686(5)	25.8542(6)
α/°	90	90
β/°	103.758(3)	90
γ/°	90	90
Volume/Å ³	2224.53(13)	2311.08(9)
Z	8	8
ρ _{calc} /g cm ⁻³	1.559	1.581
μ/mm ⁻¹	11.995	11.577
F(000)	1072	1136
Crystal size/mm ³	0.10 × 0.06 × 0.03	0.16 × 0.14 × 0.04
Radiation	CuKα (λ = 1.54178 Å)	CuKα (λ = 1.54178 Å)
2Θ range/°	10.14 to 152.31	11.43 to 152.74
Index ranges	-17 ≤ h ≤ 19, -8 ≤ k ≤ 9, -22 ≤ l ≤ 20	-12 ≤ h ≤ 10, -11 ≤ k ≤ 8, -32 ≤ l ≤ 30
Reflections collected	11907	11413
Independent reflections	4582 [R _{int} = 0.0514, R _{sigma} = 0.0571]	2400 [R _{int} = 0.0339, R _{sigma} = 0.0244]
Data/restraints/parameters	4582/1/295	2400/0/165
Goodness-of-fit on F ²	1.02	1.058
Final R indexes [I ≥ 2σ(I)]	R1 = 0.0442, wR2 = 0.1016	R1 = 0.0278, wR2 = 0.0661
Final R indexes [all data]	R1 = 0.0650, wR2 = 0.1134	R1 = 0.0336, wR2 = 0.0699
Largest diff. peak/hole/e Å ⁻³	0.67/-0.92	0.29/-0.42

	3^{Ru}	<i>anti</i> - 4^{Ru}
Empirical formula	C ₂₀ H ₂₄ Cl ₂ FeNOPRu	C ₄₀ H ₄₆ Cl ₂ Fe ₂ N ₂ O ₂ P ₂ Ru ₂
Formula weight	553.19	1033.47
Temperature/K	120(2)	120(2)
Crystal system	monoclinic	triclinic
Space group	<i>P</i> 2 ₁ /c	<i>P</i> -1
a/Å	20.2447(8)	7.6871(4)
b/Å	9.5396(4)	11.1384(6)
c/Å	10.8062(4)	11.9077(6)
α/°		78.737(2)
β/°	94.591(2)	84.523(2)
γ/°		83.307(2)
Volume/Å ³	2080.3(1)	990.34(9)
Z	4	1
ρ _{calc} /g cm ⁻³	1.766	1.733
μ/mm ⁻¹	1.768	1.719
F(000)	1112	520
Crystal size/mm ³	0.18 × 0.17 × 0.04	0.13 × 0.11 × 0.04
Radiation	MoKα (λ = 0.71073 Å)	MoKα (λ = 0.71073 Å)
2Θ range/°	2.36 to 27.54	2.31 to 27.46
Index ranges	-26 ≤ h ≤ 26, -12 ≤ k ≤ 12, -13 ≤ l ≤ 14	-9 ≤ h ≤ 96, -14 ≤ k ≤ 14, -15 ≤ l ≤ 15
Reflections collected	44034	21236
Independent reflections	4784 [R _{int} = 0.0331, R _{sigma} = 0.0171]	4552 [R _{int} = 0.0402, R _{sigma} = 0.0340]
Data/restraints/parameters	4784/0/247	4552/6/239
Goodness-of-fit on F ²	1.06	1.09
Final R indexes [I ≥ 2σ(I)]	R1 = 0.0199, wR2 = 0.0443	R1 = 0.0292, wR2 = 0.0581
Final R indexes [all data]	R1 = 0.0256, wR2 = 0.0463	R1 = 0.0412, wR2 = 0.0612
Largest diff. peak/hole/e Å ⁻³	0.53/-0.72	1.08/-0.62

	<i>syn</i> - 4 ^{Rh}	<i>anti</i> - 4 ^{Rh}
Empirical formula	C ₄₂ H ₅₂ Cl ₂ Fe ₂ N ₂ O ₂ P ₂ Rh ₂	C ₄₂ H ₅₂ Cl ₂ Fe ₂ N ₂ O ₂ P ₂ Rh ₂
Formula weight	1067.21	1067.21
Temperature/K	120(2)	150(2)
Crystal system	monoclinic	monoclinic
Space group	<i>C</i> 2/c	<i>P</i> 2 ₁ /c
a/Å	25.6521(7)	11.0602(3)
b/Å	9.0610(2)	14.4369(4)
c/Å	20.9168(6)	13.1738(4)
α/°		
β/°	119.129(1)	92.044(1)
γ/°		
Volume/Å ³	4234(4)	2102.2(1)
Z	4	2
ρ _{calc} /g cm ⁻³	1.674	1.686
μ/mm ⁻¹	1.677	1.689
F(000)	2160	1080
Crystal size/mm ³	0.19 × 0.15 × 0.11	0.51 × 0.24 × 0.21
Radiation	MoKα (λ = 0.71073 Å)	MoKα (λ = 0.71073 Å)
2Θ range/°	2.24 to 27.48	2.32 to 27.51
Index ranges	-33 ≤ h ≤ 33, -11 ≤ k ≤ 11, -27 ≤ l ≤ 27	-14 ≤ h ≤ 14, -18 ≤ k ≤ 18, -14 ≤ l ≤ 17
Reflections collected	30944	30792
Independent reflections	4866 [R _{int} = 0.0284, R _{sigma} = 0.0189]	4851 [R _{int} = 0.0360, R _{sigma} = 0.0238]
Data/restraints/parameters	4866/0/249	4851/0/249
Goodness-of-fit on F ²	1.05	1.11
Final R indexes [I ≥ 2σ(I)]	R1 = 0.0194, wR2 = 0.0448	R1 = 0.0458, wR2 = 0.1153
Final R indexes [all data]	R1 = 0.0241, wR2 = 0.0468	R1 = 0.0560, wR2 = 0.1221
Largest diff. peak/hole/e Å ⁻³	0.40/-0.62	1.85/-0.89

3. Spectra for the reported compounds

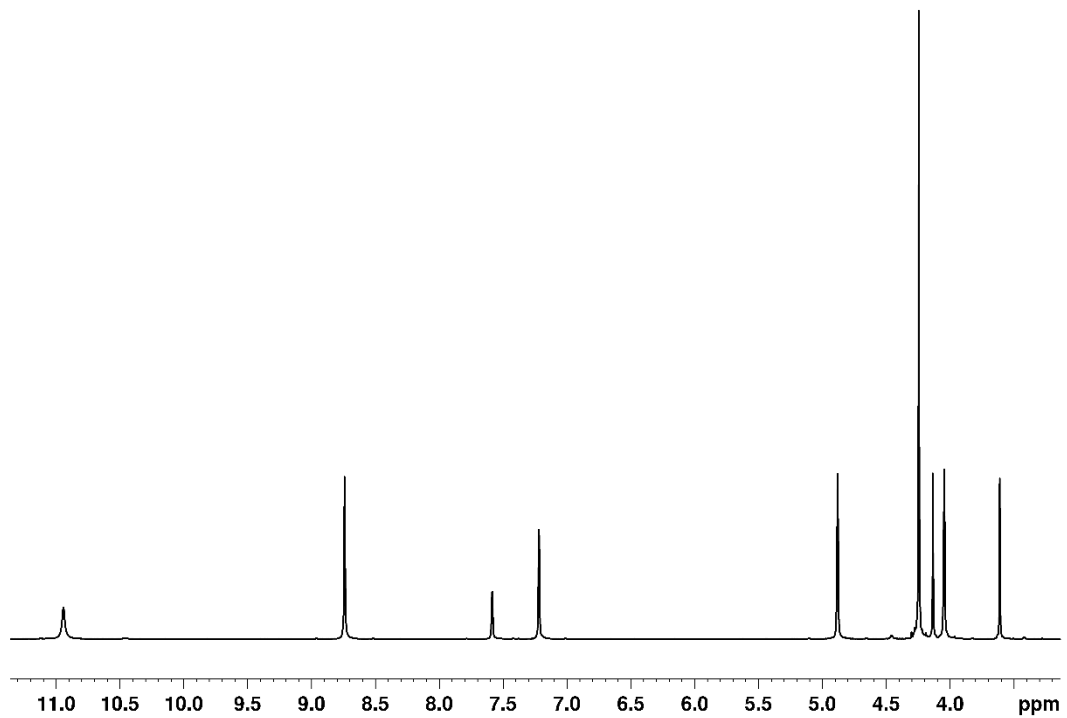


Figure S10. ^1H NMR spectrum of a pyridine-d₅ solution of **1**.

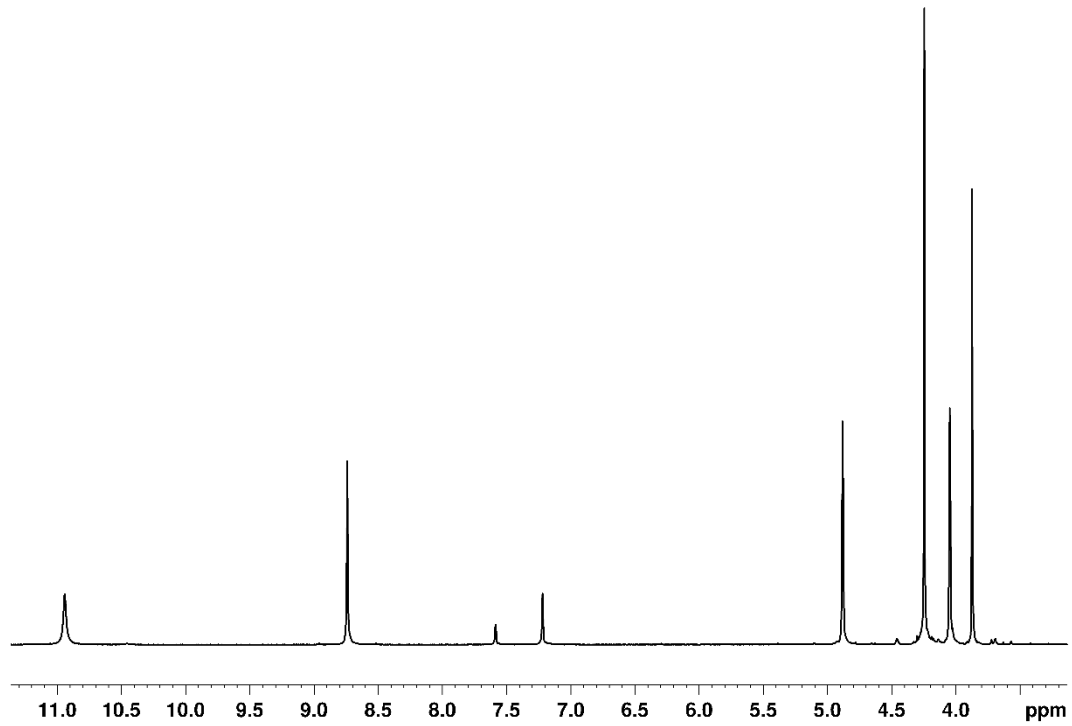


Figure S11. $^1\text{H}\{^{31}\text{P}\}$ NMR spectrum of a pyridine-d₅ solution of **1**.

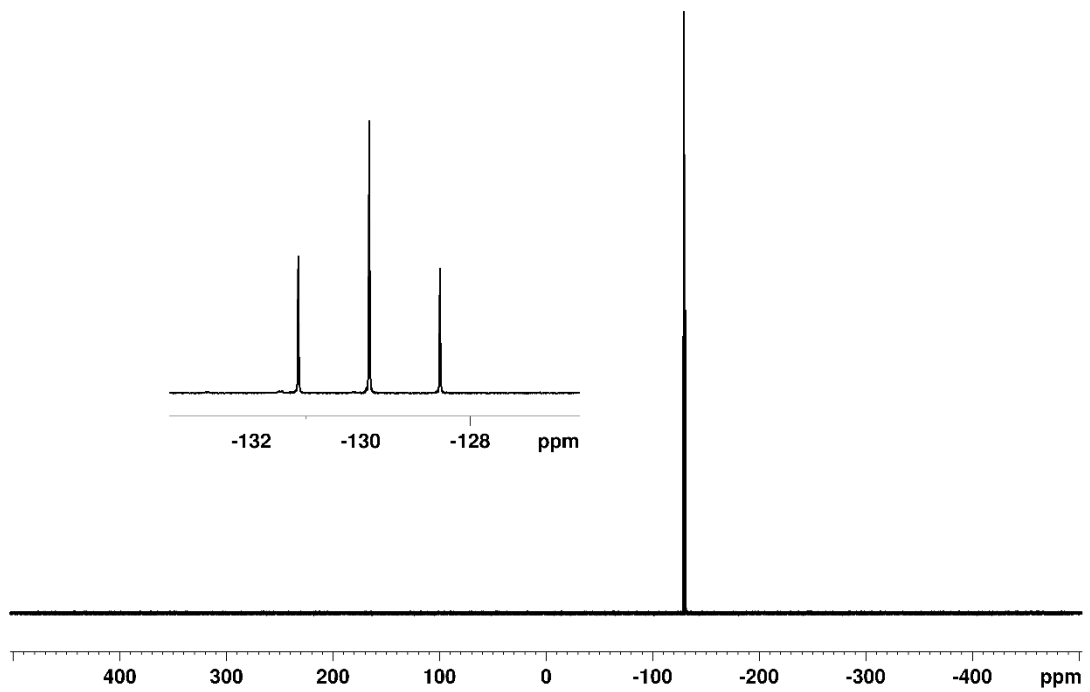


Figure S12. ^{31}P NMR spectrum of a pyridine- d_5 solution of **1**.

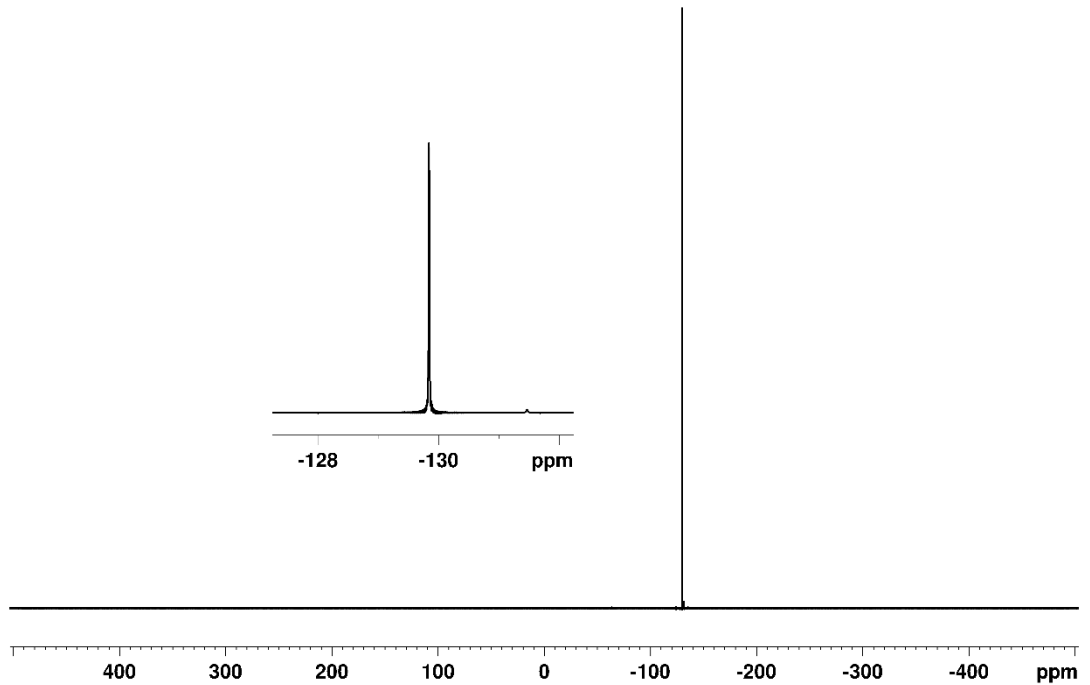


Figure S13. $^{31}\text{P}\{\text{H}\}$ NMR spectrum of a pyridine- d_5 solution of **1**.

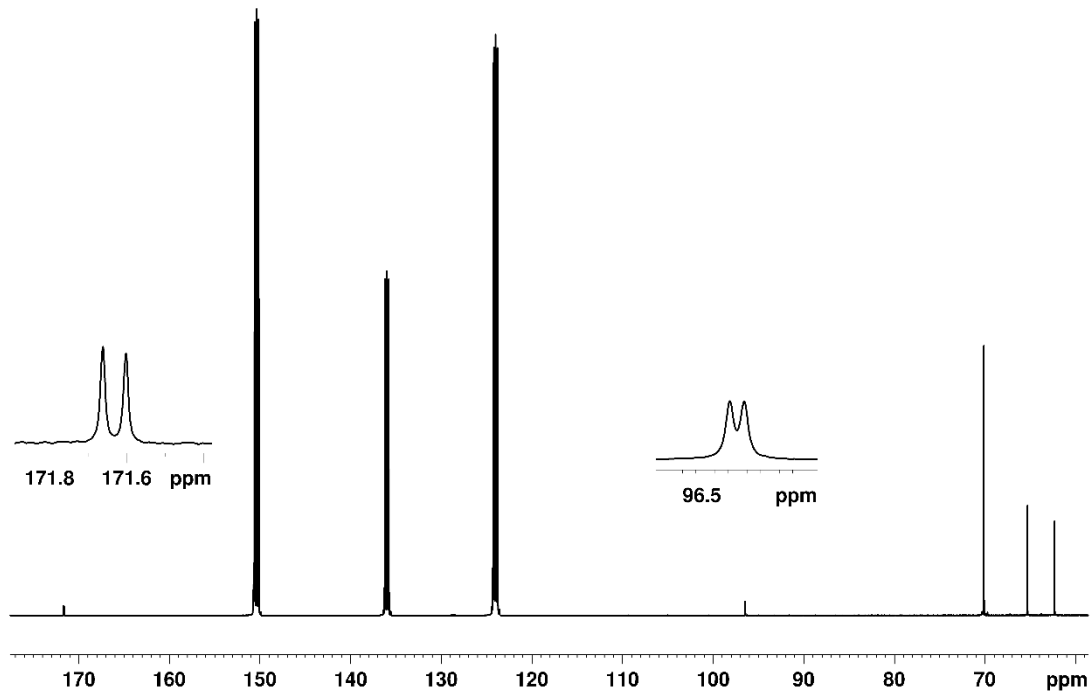


Figure S14. $^{13}\text{C}\{^1\text{H}\}$ NMR spectrum of a pyridine- d_5 solution of **1**.

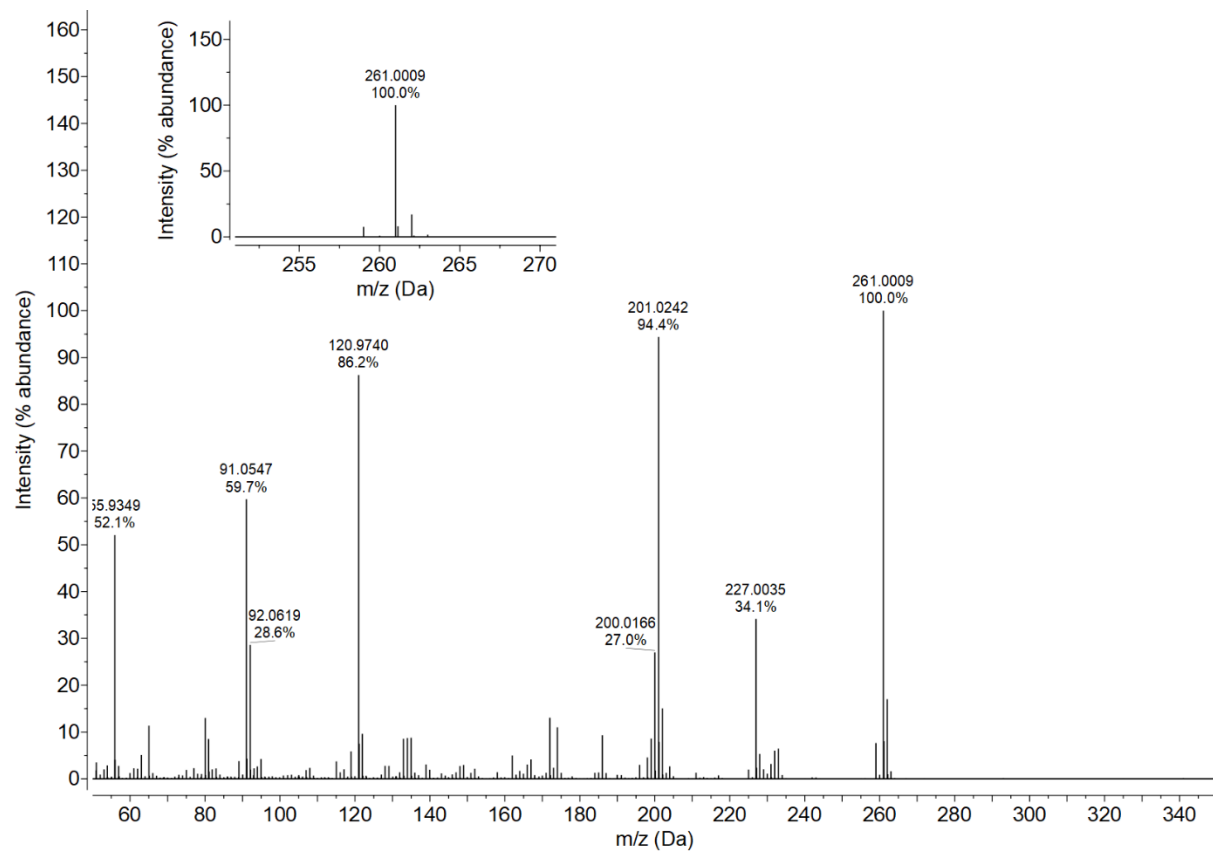


Figure S15. Positive ion mode EI MS spectrum of **1** (inset shows the molecular ion – $\text{C}_{11}\text{H}_{12}\text{FeNOP}$, calc. 261.0006).

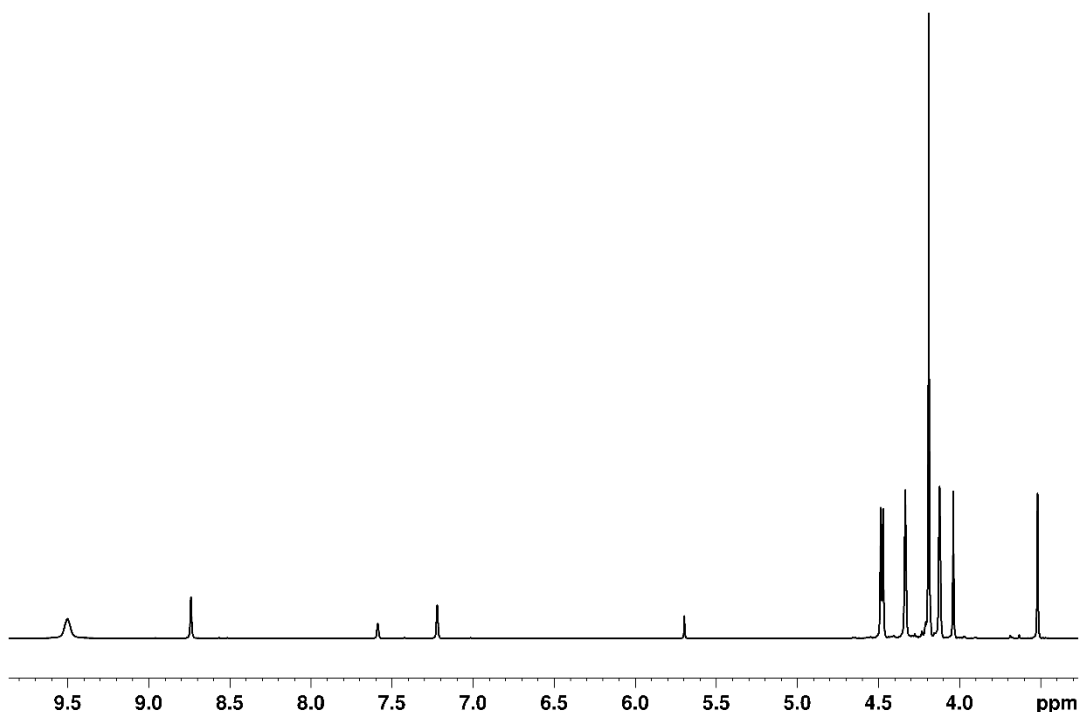


Figure S16. ¹H NMR spectrum of a pyridine-d₅ solution of **2**.

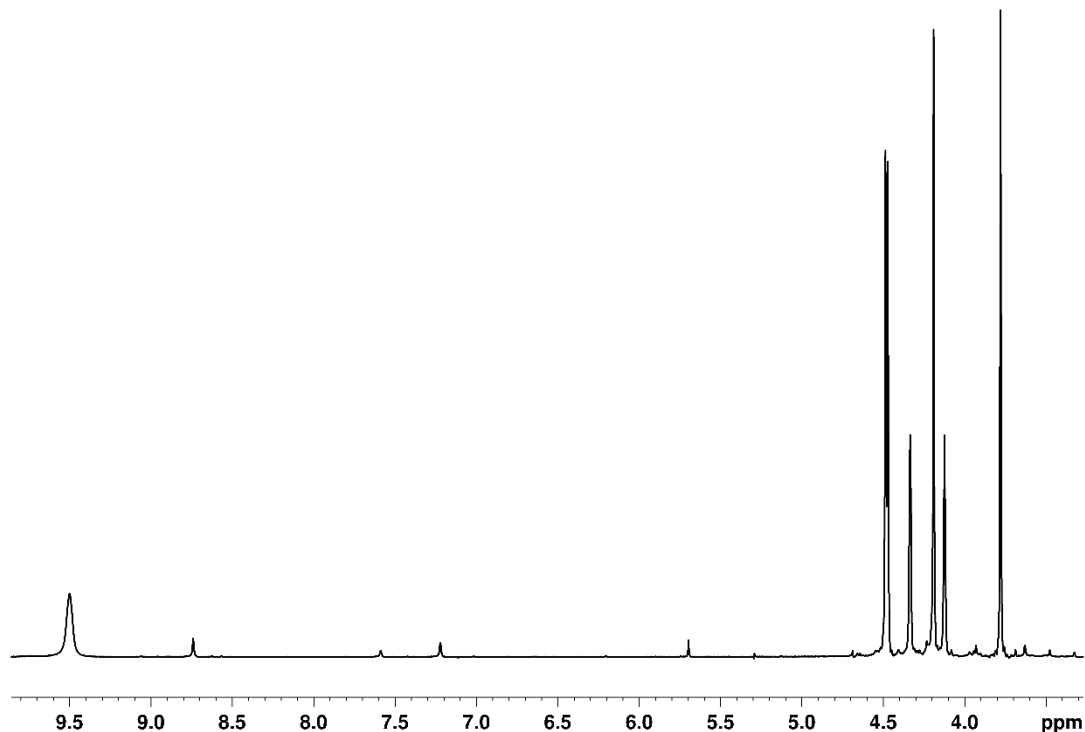


Figure S17. ¹H{³¹P} NMR spectrum of a pyridine-d₅ solution of **2**.

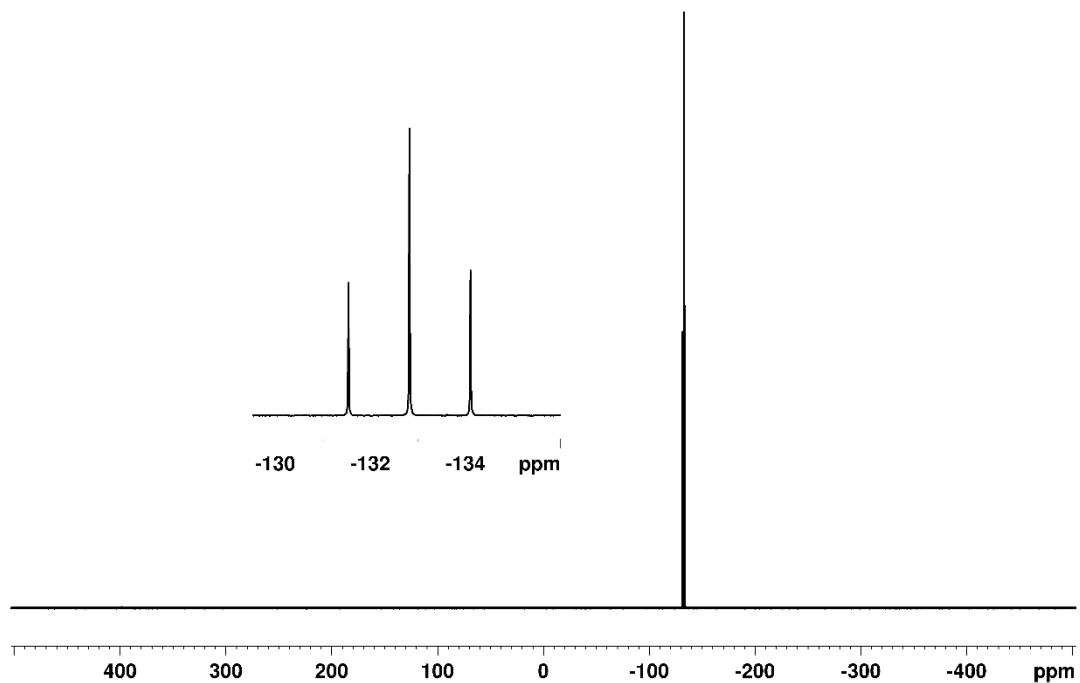


Figure S18. ^{31}P NMR spectrum of a pyridine- d_5 solution of **2**.

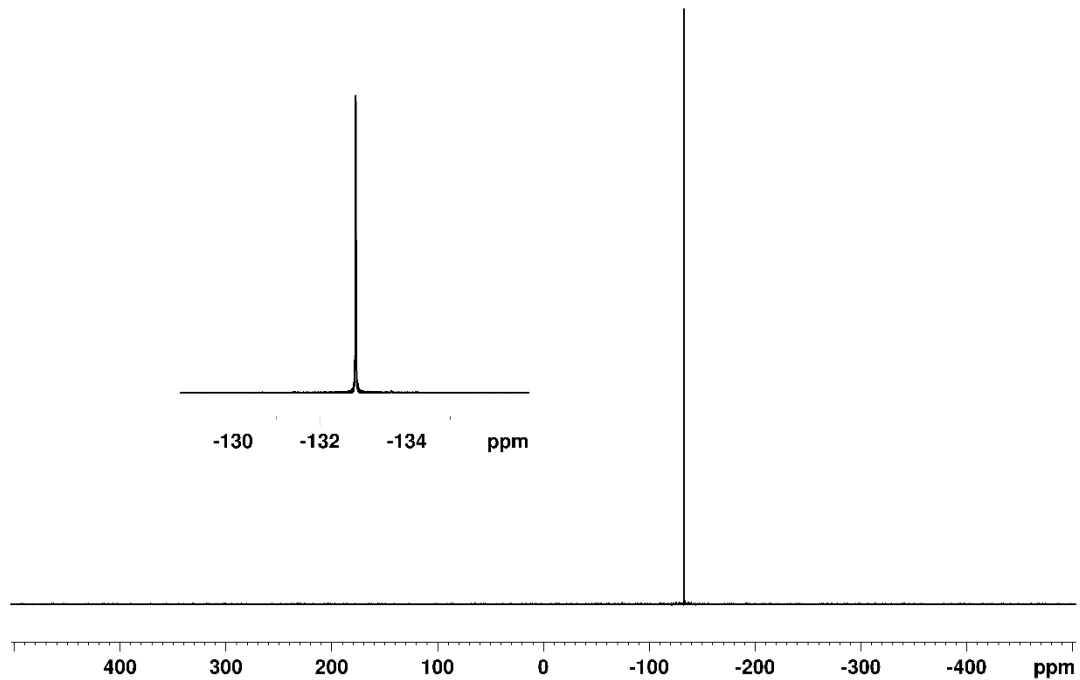


Figure S19. $^{31}\text{P}\{\text{H}\}$ NMR spectrum of a pyridine- d_5 solution of **2**.

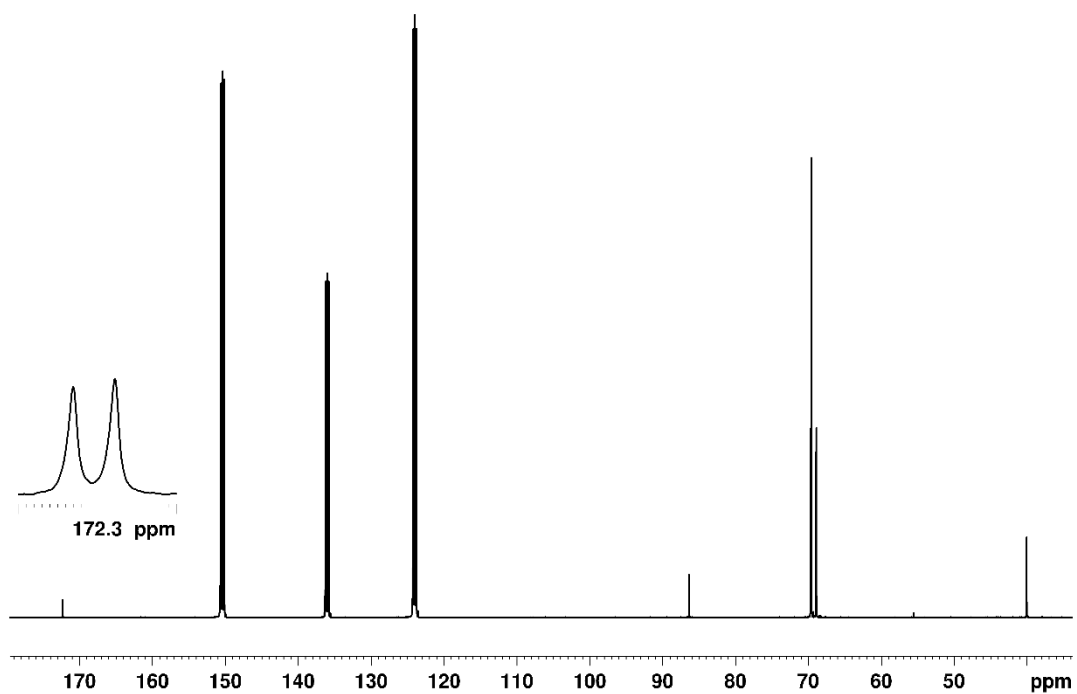


Figure S20. $^{13}\text{C}\{^1\text{H}\}$ NMR spectrum of a pyridine- d_5 solution of **2**.

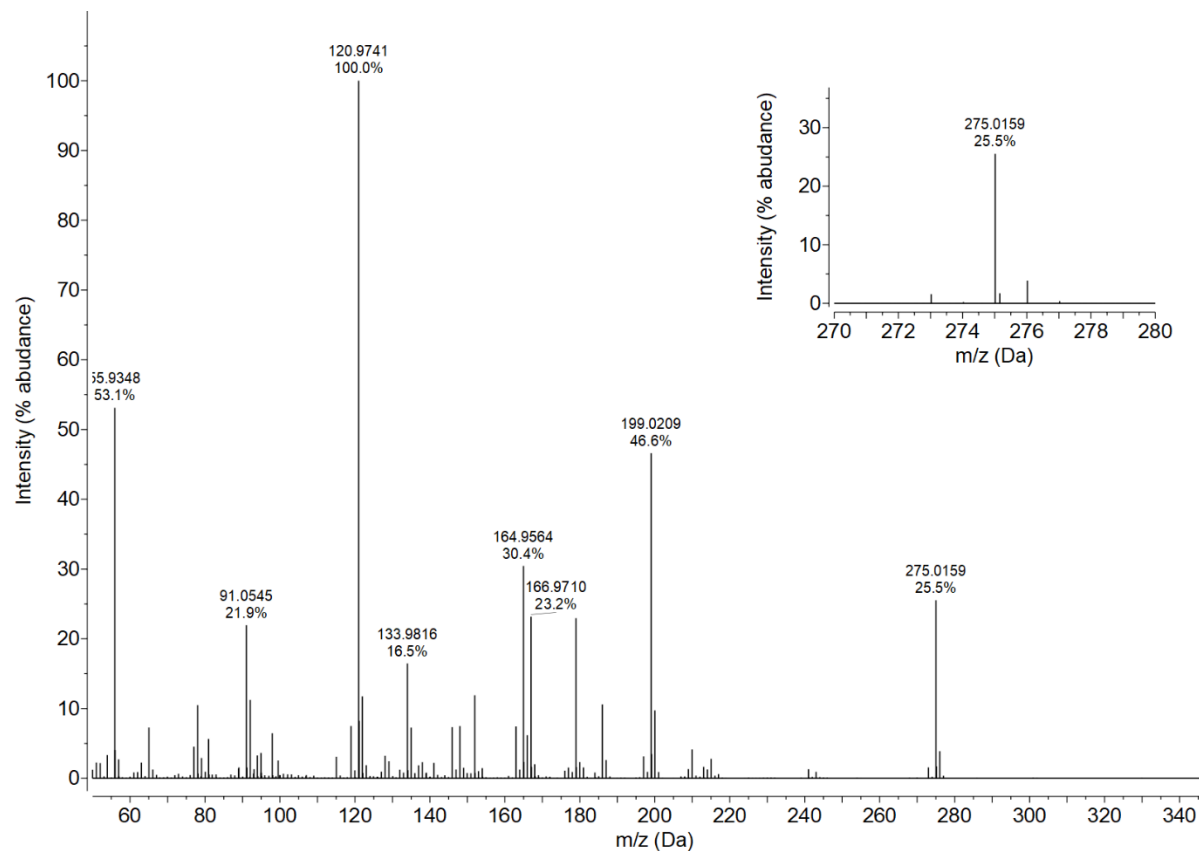


Figure S21. Positive-ion mode EI MS spectrum of **2** (inset shows the molecular ion – $\text{C}_{12}\text{H}_{14}\text{FeNOP}$, calc. 275.0162).

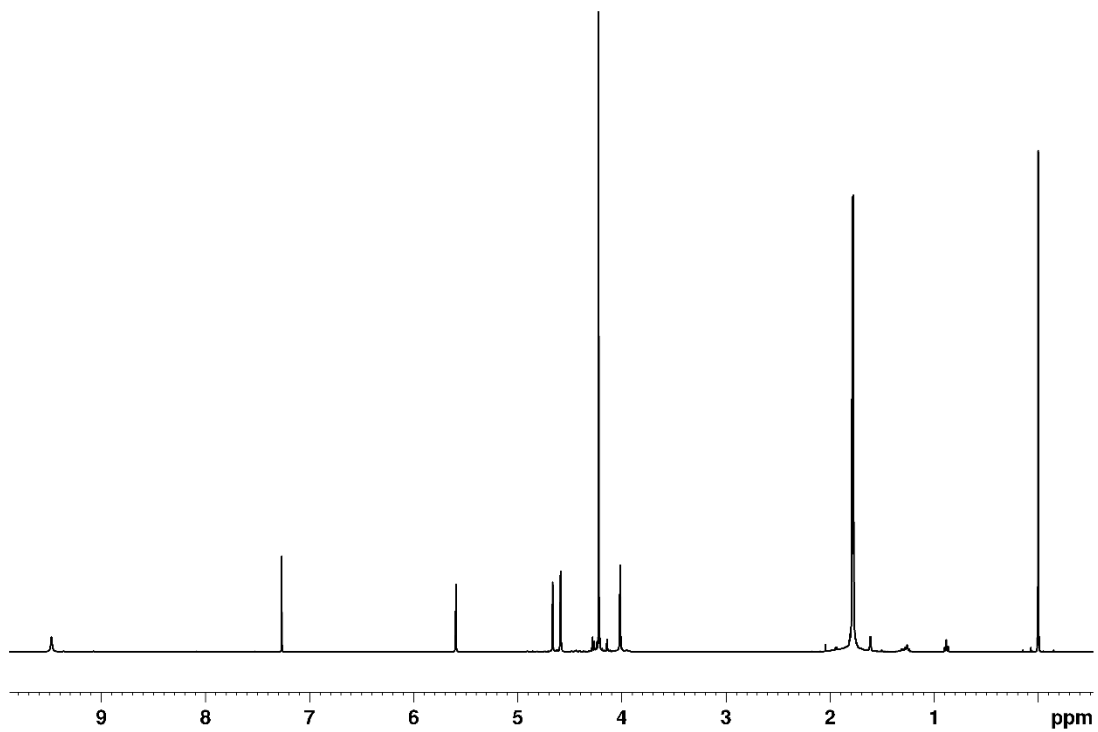


Figure S22. ¹H NMR spectrum of a CDCl₃ solution of **3^{Rh}**.

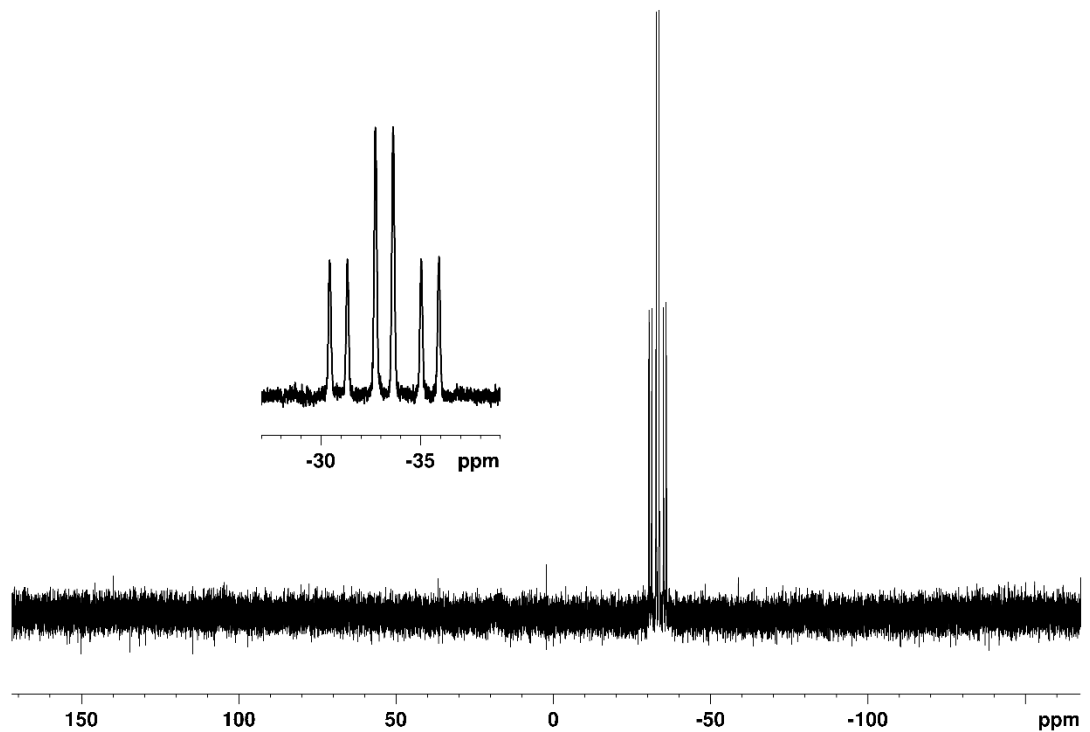


Figure S23: ³¹P NMR spectrum of a CDCl₃ solution of **3^{Rh}**.

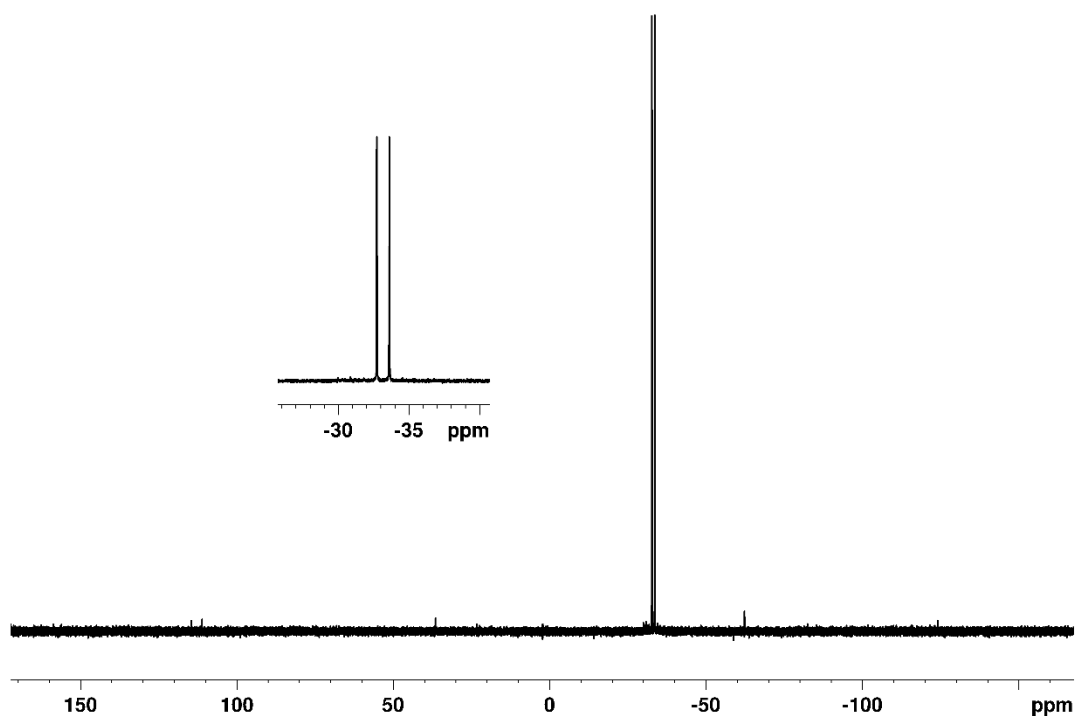


Figure S24. $^{31}\text{P}\{\text{H}\}$ NMR spectrum of a CDCl_3 solution of $\mathbf{3}^{\text{Rh}}$.

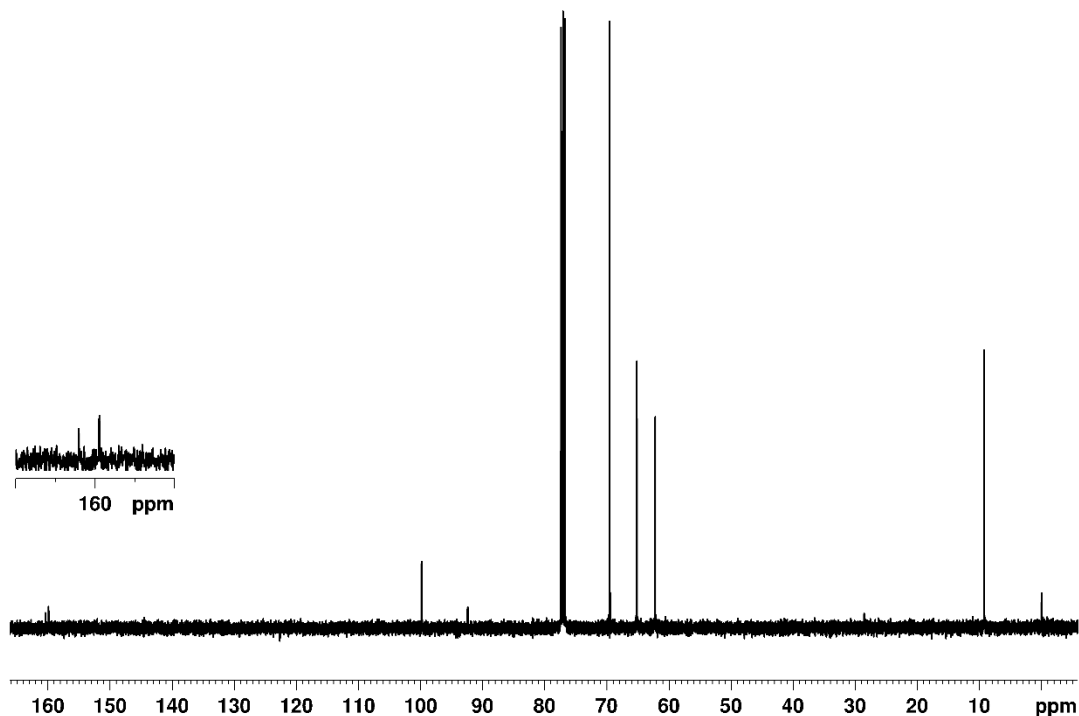


Figure S25. $^{13}\text{C}\{\text{H}\}$ NMR spectrum of a CDCl_3 solution of $\mathbf{3}^{\text{Rh}}$.

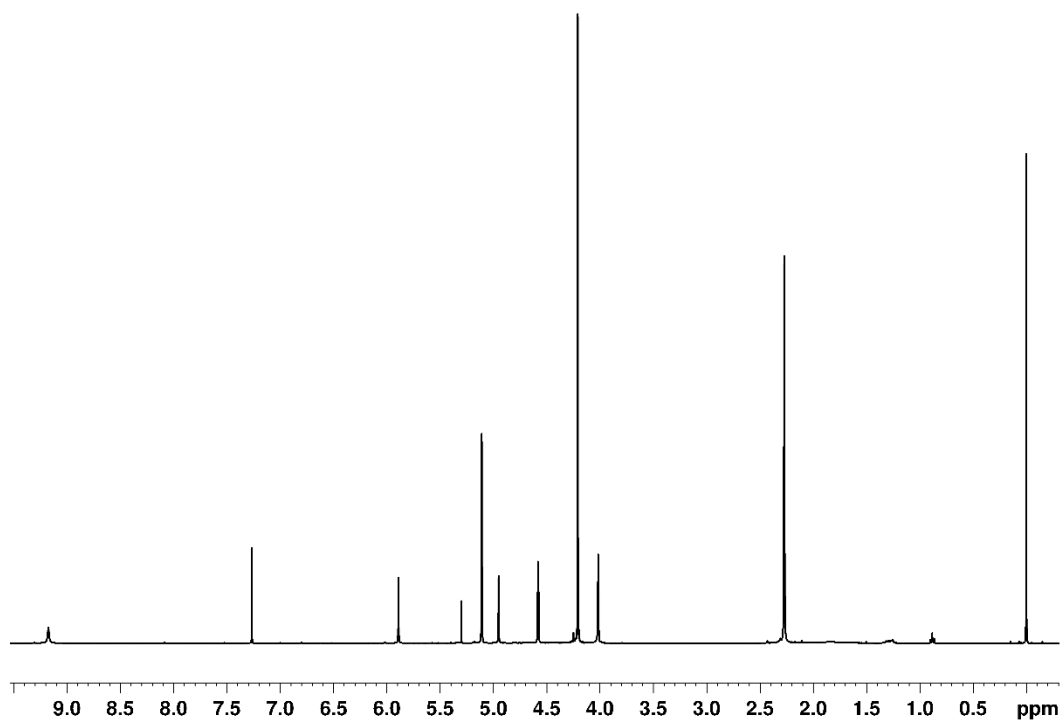


Figure S26. ¹H NMR spectrum of a CDCl₃ solution of 3^{Ru}.

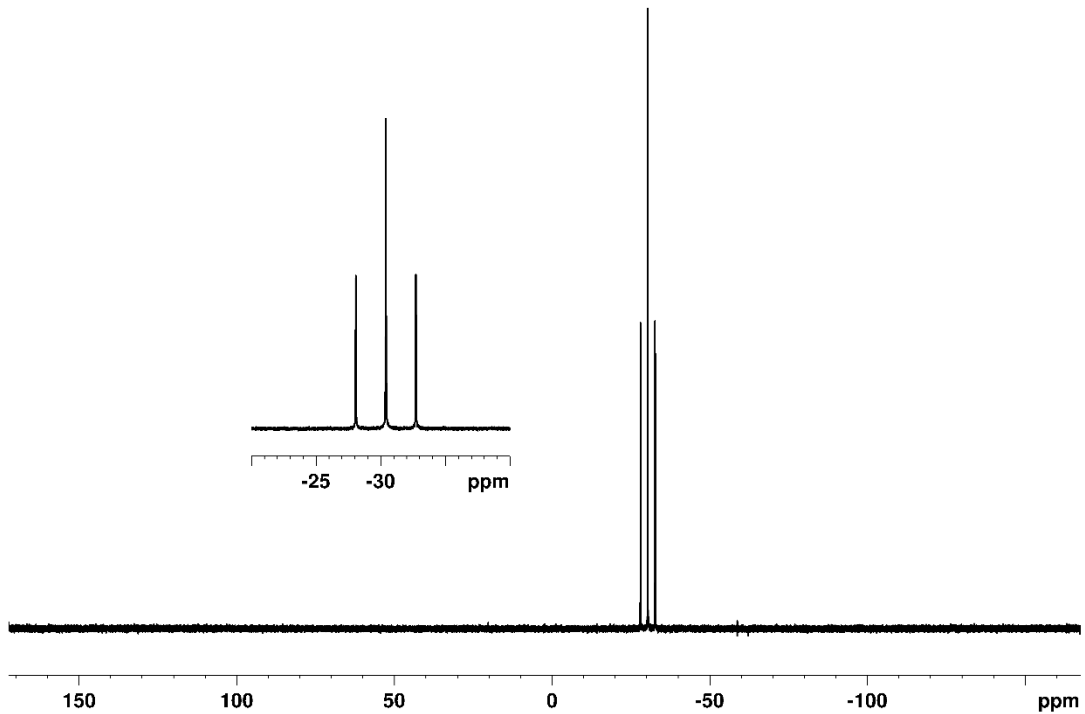


Figure S27. ³¹P NMR spectrum of a CDCl₃ solution of 3^{Ru}.

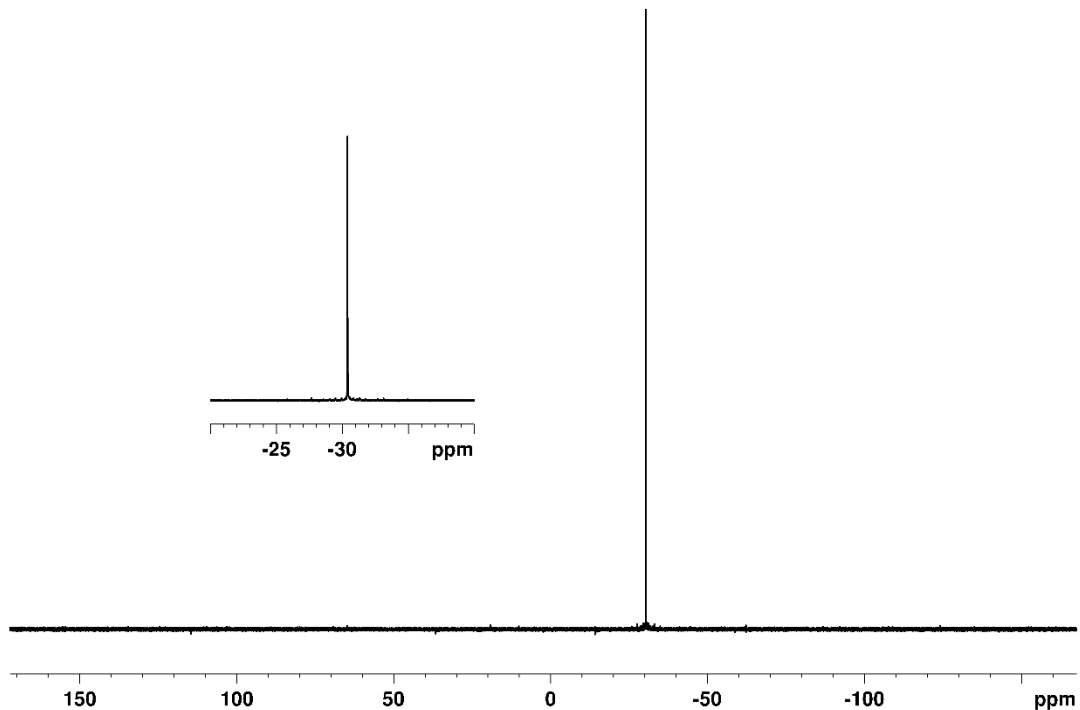


Figure S28. $^{31}\text{P}\{\text{H}\}$ NMR spectrum of a CDCl_3 solution of $\mathbf{3}^{\text{Ru}}$.

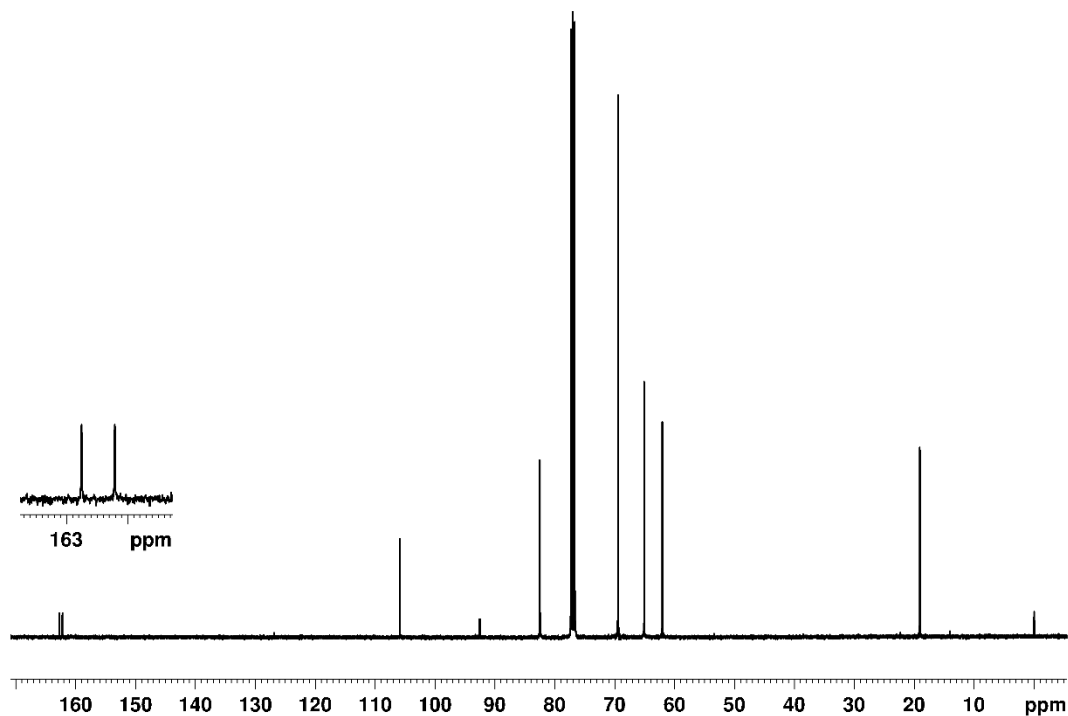


Figure S29. $^{13}\text{C}\{\text{H}\}$ NMR spectrum of a CDCl_3 solution of $\mathbf{3}^{\text{Ru}}$.

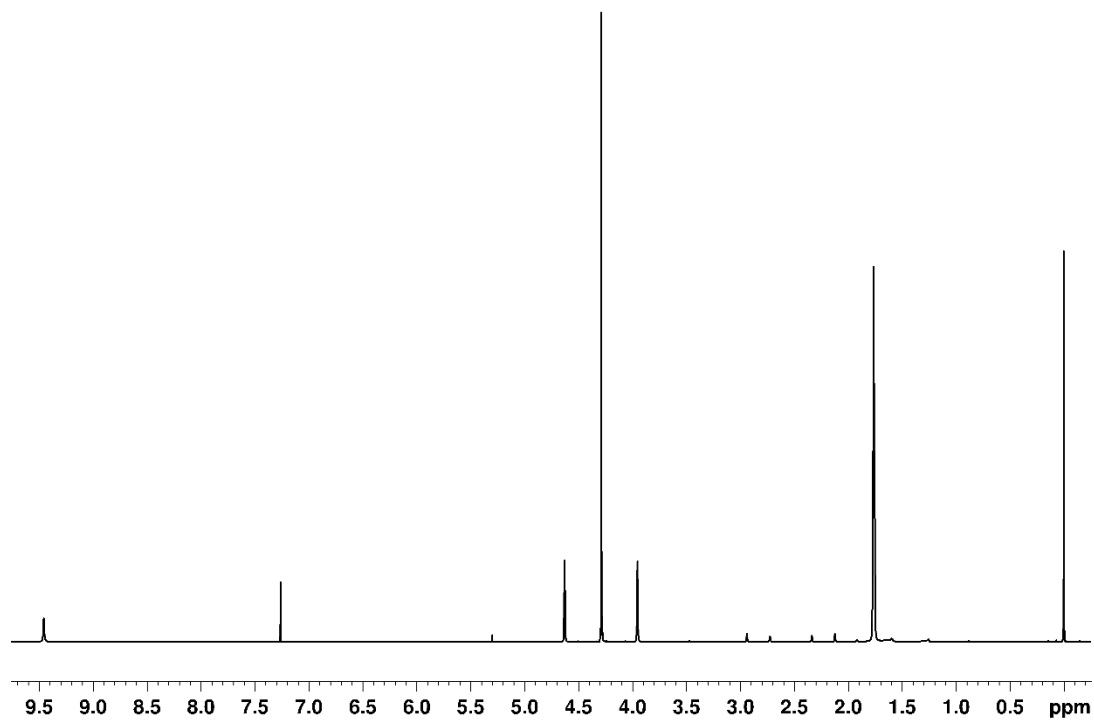


Figure S30. ¹H NMR spectrum of a CDCl₃ solution of *anti*-4^{Rh}.

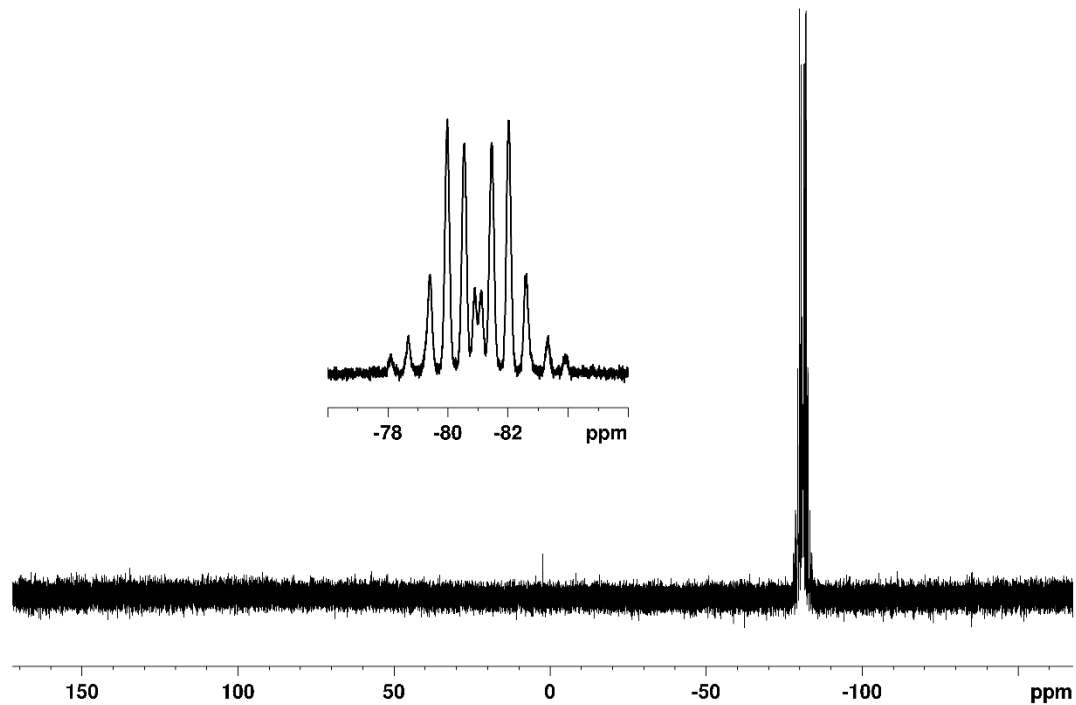


Figure S31. ³¹P NMR spectrum of a CDCl₃ solution of *anti*-4^{Rh}.

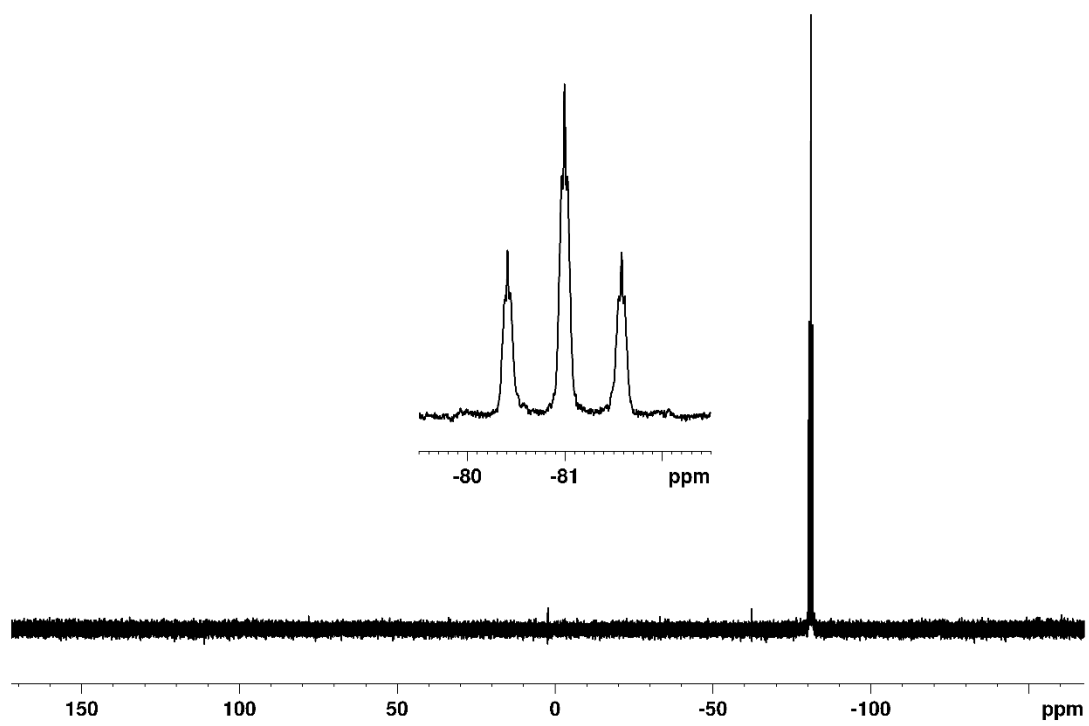


Figure S32. $^{31}\text{P}\{\text{H}\}$ NMR spectrum of a CDCl_3 solution of *anti*- $\textbf{4}^{\text{Rh}}$.

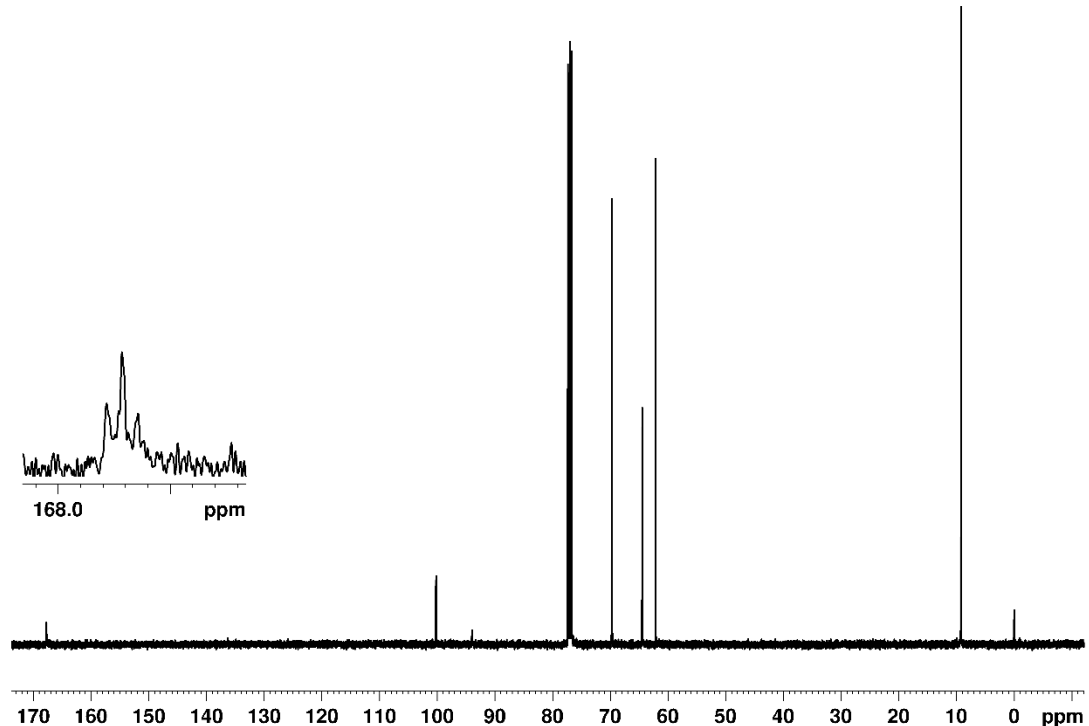


Figure S33. $^{13}\text{C}\{\text{H}\}$ NMR spectrum of a CDCl_3 solution of *anti*- $\textbf{4}^{\text{Rh}}$.

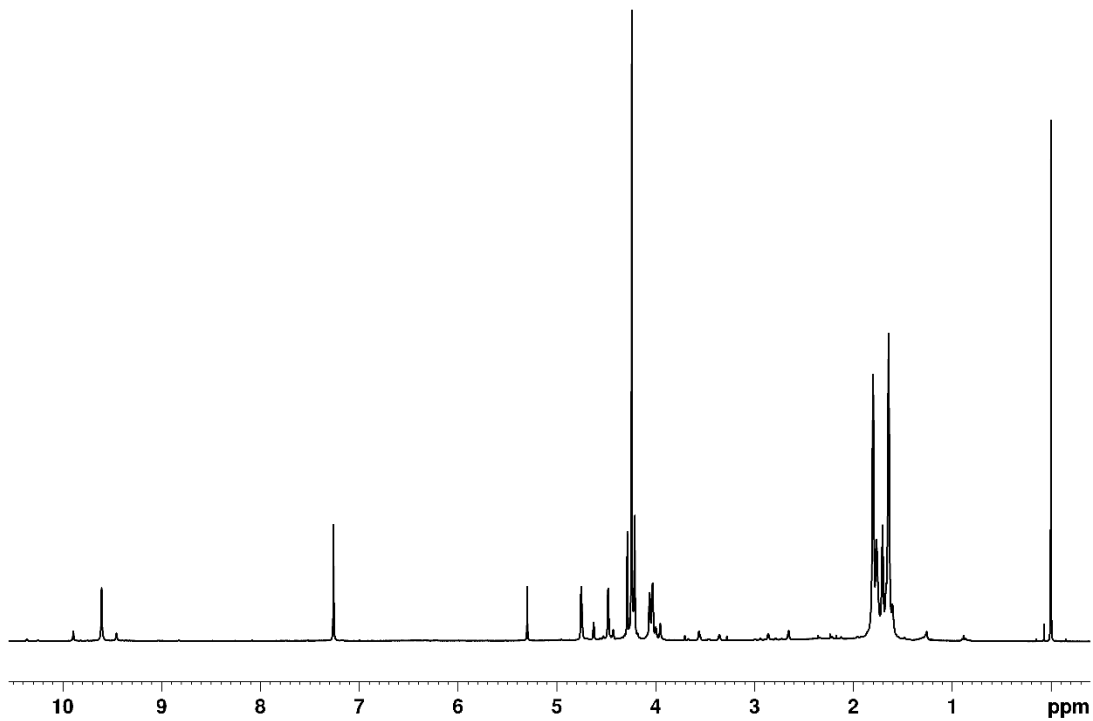


Figure S34. ¹H NMR spectrum of a CDCl₃ solution of the reaction mixture obtained mixing **1** with [(η^5 -C₅Me₅)RhCl(μ -Cl)]₂ and standing for 1 d, which contains *syn*- and *anti*-**4**^{Rh}.

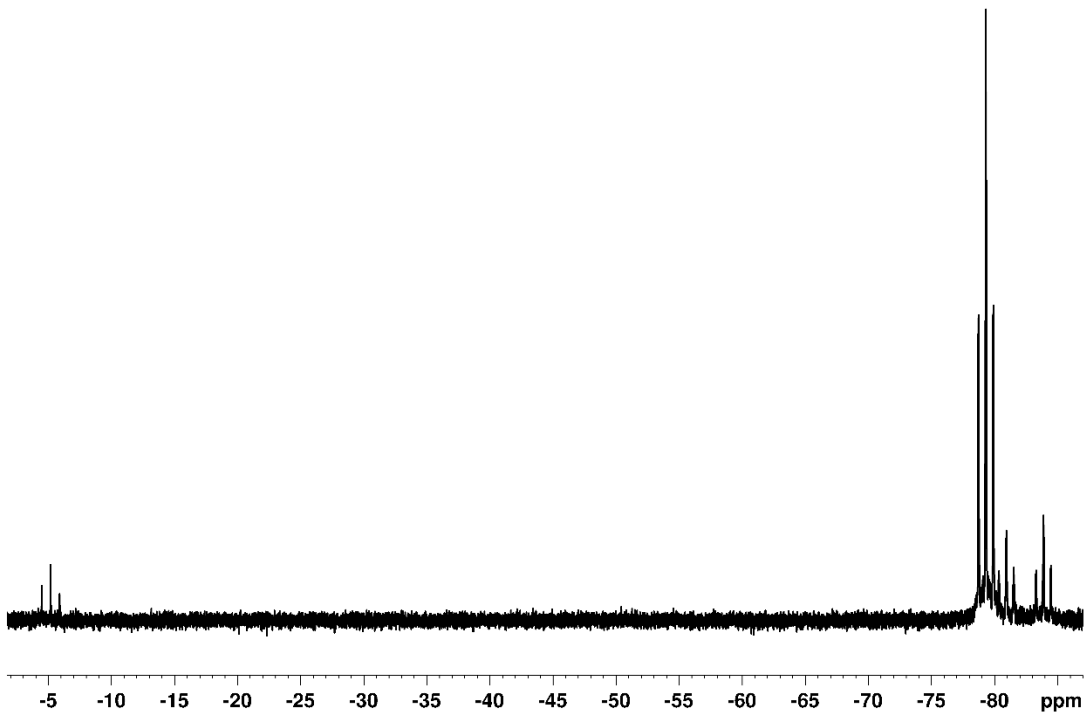


Figure S35. ³¹P{¹H} NMR spectrum of a CDCl₃ solution of the reaction mixture obtained after adding **1** to [(η^5 -C₅Me₅)RhCl(μ -Cl)]₂ and standing for 1 d, which contains *syn*- and *anti*-**4**^{Rh}.

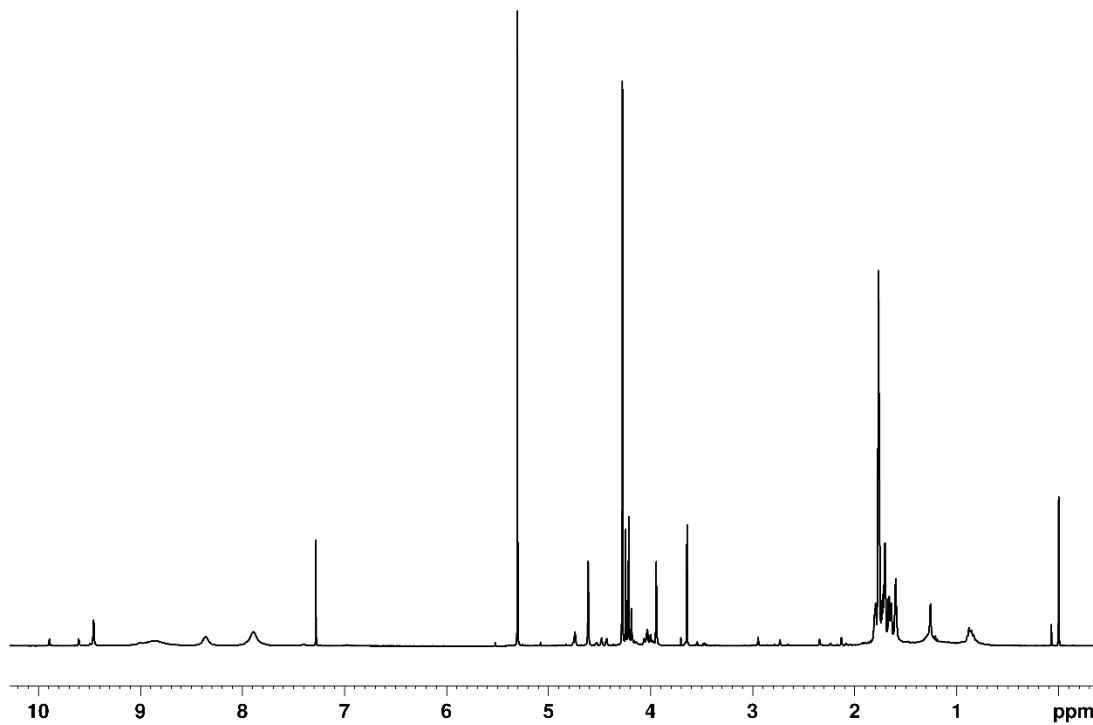


Figure S36. $\{^1\text{H}\}$ NMR spectrum of a CDCl_3 solution of the reaction mixture obtained after adding **1** and pyridine to $[(\eta^5\text{-C}_5\text{Me}_5)\text{RhCl}(\mu\text{-Cl})]_2$ and standing for 1 d, which contains mainly *anti*-**4^{Rh}.**

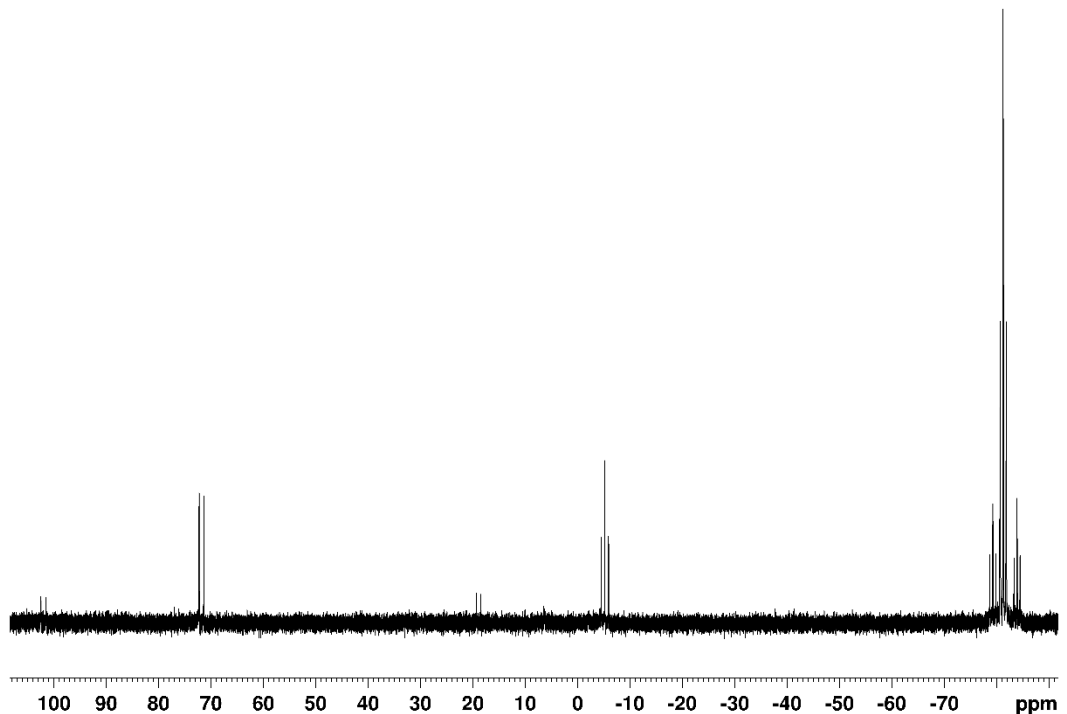


Figure S37. $^{31}\text{P}\{^1\text{H}\}$ NMR spectrum of a CDCl_3 solution of the reaction mixture obtained after adding **1** and pyridine to $[(\eta^5\text{-C}_5\text{Me}_5)\text{RhCl}(\mu\text{-Cl})]_2$ and standing for 1 d, which contains mainly *anti*-**4^{Rh}.**

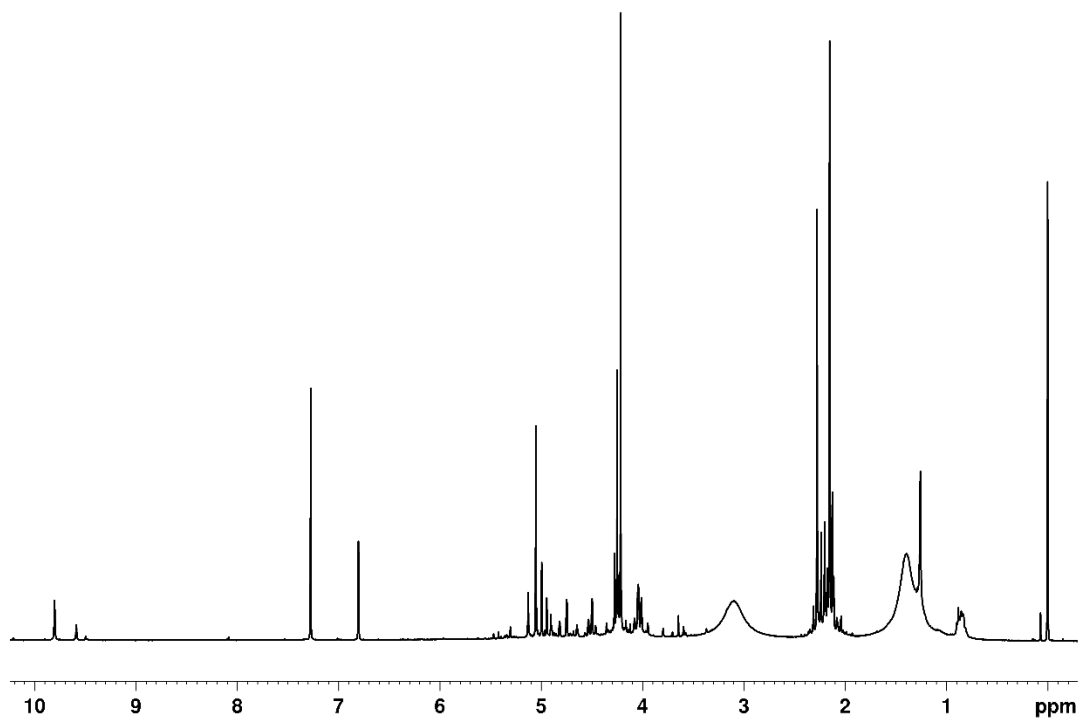


Figure S38. ¹H NMR spectrum (CDCl_3) of the reaction mixture obtained after adding **1** and triethylamine to $[(\eta^6\text{-mes})\text{RuCl}(\mu\text{-Cl})]_2$ and standing for 1 d.

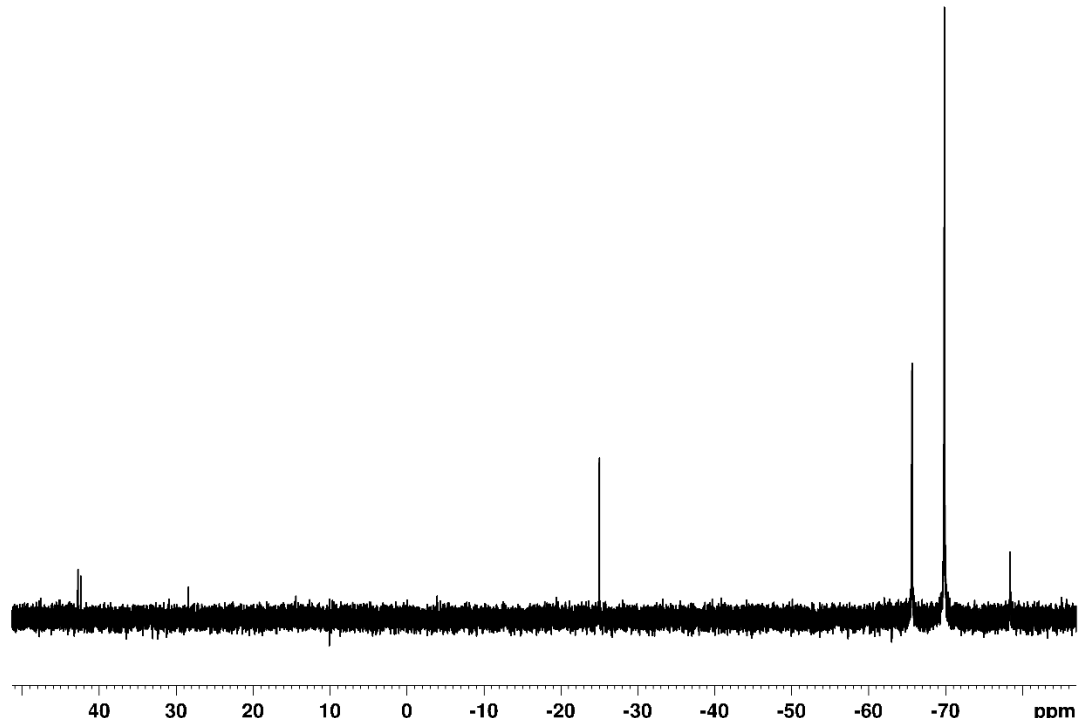


Figure S39. ³¹P{¹H} NMR spectrum of a CDCl_3 solution of the reaction mixture obtained after adding **1** and triethylamine to $[(\eta^6\text{-mes})\text{RuCl}(\mu\text{-Cl})]_2$ and standing for 1 d.